

Evaluation of neutron radiation field in carbon ion therapy

Jun-Kui Xu(徐俊奎)^{1,2;1)} You-Wu Su(苏有武)² Wu-Yuan Li(李武元)² Wei-Wei Yan(严维伟)²
 Xi-Meng Chen(陈熙萌)¹ Wang Mao(毛旺)² Cheng-Guo Pang(庞成果)¹

¹ School of Nuclear Science and Technology, Lanzhou University, Lanzhou 730000, China

² Institute of Modern Physics, Chinese Academy of Science, Lanzhou 730000, China

Abstract: Carbon ions have significant advantages in tumor therapy because of their physical and biological properties. In view of the radiation protection, the safety of patients is the most important issue in therapy processes. Therefore, the effects of the secondary particles produced by the carbon ions in the tumor therapy should be carefully considered, especially for the neutrons. In the present work, the neutron radiation field induced by carbon ions was evaluated by using the FLUKA code. The simulated results of neutron energy spectra and neutron dose was found to be in good agreement with the experiment data. In addition, energy deposition of carbon ions and neutrons in tissue-like media was studied, it is found that the secondary neutron energy deposition is not expected to exceed 1% of the carbon ion energy deposition in a typical treatment.

Keywords: neutron radiation, radiation protection, energy deposition

PACS: 07.89.+b, 28.41.Qb, 29.25.Dz **DOI:** 10.1088/1674-1137/40/1/018201

1 Introduction

Heavy ion cancer therapy has been developing rapidly in recent years because of its physical and biological characteristics. It is known that heavy ions with certain energies have a fixed range in the target and a typical Bragg peak presents. Therefore the position of this Bragg peak can be easily controlled [1]. Taking the patient safety into account the effects of secondary particles caused by heavy ion reactions must be carefully considered in cancer therapy. At a heavy ion accelerator, various kinds of secondary particles are created through nuclear reaction of the heavy ions with the accelerator components or target. Neutrons are the most abundant products in all secondary particles. Moreover, because the neutrons cannot cause ionization directly, they may affect a large area. In the cancer therapy, it means that the neutrons would influence the whole body of a patient including both tumor and healthy tissue. Therefore, neutrons are the most important factor needed to take consideration both in safety evaluations of heavy ion therapy and in the environmental shielding of the accelerator facilities. The neutron energy spectra is a fundamental measurable quantity which is needed in the radiation protection of a accelerator. The neutron dose can be obtained through the neutron energy spectra and the dose conversion coefficients given by the International Commission of Radiological Protection (ICRP) [2].

The effects of the secondary particles produced during radiotherapy has been intensively investigated in past years [3, 4]. In addition, there have been a number of previous studies on the neutron yields, neutron spectra and angular distributions. The high energy neutron spectra and angular distribution of carbon ions stopping in a thick copper target was studied by T. Nakamura at HIMAC (Heavy Ion Medical Accelerator in Chiba) in 1999 [5]. More studies of neutron yields of heavy ions hitting a thick target were studied in Refs. [6, 7]. In our previous work, neutron fluence and angular distributions were measured around a thick target bombarded by 50-100 MeV/u ¹⁸O ions using an activation method at the Heavy Ion Research Facility in Lanzhou (HIRFL) in 1999 [8]. In a 100 MeV/u carbon ion therapy, the neutron dose distribution was measured in a superficial tumor treatment terminal at HIRFL in 2010 [9]. With the development of heavy ion radiotherapy applications, two HIMMs (Heavy Ion Medical Machines) are currently being built in Lanzhou and Wuwei, Gansu, China, respectively. The details of such facilities are described in a previous article [10]. For the patient safety, it is significant to evaluate the neutron radiation field during the carbon ion therapy.

In the present work, the secondary neutron energy spectra around a thick target bombarded by carbon ions was studied using a Monte Carlo program code. The simulated results indicate that the energy spectra is in

Received 18 March 2015

1) E-mail: xujunkui@impcas.ac.cn

©2016 Chinese Physical Society and the Institute of High Energy Physics of the Chinese Academy of Sciences and the Institute of Modern Physics of the Chinese Academy of Sciences and IOP Publishing Ltd

good agreement with previous experimental data. In addition, the distribution of the neutron dose was also calculated. We attempt to provide a full set of numerical data, which can be directly employed both for shielding design of high-energy ion accelerators and for evaluating the safety of the patient during a treatment process. Further, the neutron flux distribution in the tissue-like media and the surrounding space was then studied. The results show that the neutron energy deposition in the tissue-like media does not exceed 1% of the carbon ion energy deposition.

2 Monte Carlo calculation and experiments

There are many Monte Carlo transport programs available for use in the design of the radiation protection and other fields. FLUKA [11, 12] is a typical Monte Carlo code which is released as free software. In this code, the nucleus–nucleus interaction was described by the Dual Parton Model (DPM) [13] for ion energies over 5 GeV/u, the Relativistic Quantum Molecular Dynamics Model (RQMD) [14] for energies from 0.1 GeV/u to 5 GeV/u and the Boltzmann Master Equation (BME) [15] theory for energies below 0.1 GeV/u, respectively.

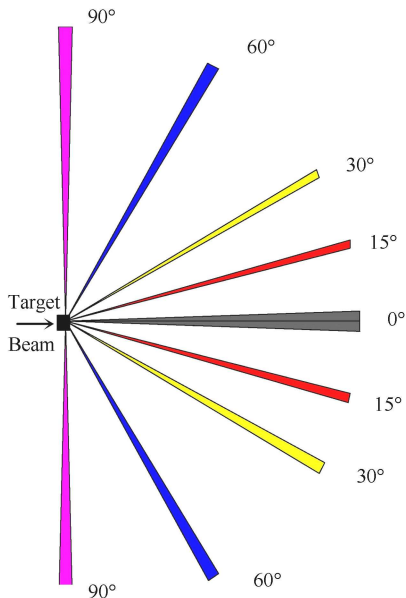


Fig. 1. (color online) Schematic diagram of simulation model.

Figure 1 shows a schematic diagram of the simulation model. Both the diameter and the thickness of the copper target is 5 cm. Its axis coincides with the beam-line. The water tissue-like target size is 30 cm \times 30 cm \times 30 cm. The composition of this tissue-like target is listed in Table 1. The size of the treatment room filled with dry air is 4 m \times 6 m \times 6 m. In the present work, the

simulation geometry only includes the shielding wall and the target, other accessories are ignored for simplification. The beam cross section diameter is 2 mm. The copper target is bombarded by carbon ions with energy of 400 MeV/u, and the tissue-like target is bombarded by carbon ions with energy of 430 MeV/u. Here, the selected ion energies and the target are consistent with the previous experimental data. In the process of our simulation, the PHSICS card was used to select the appropriate physical model. The USRBDX card is used to obtain the neutron energy spectra and the USRBIN card is chosen to obtain the neutron dose and energy deposition. FLUKA version 2011.2c was used in the present work.

Table 1. Composition of tissue-like target.

component	proportion (%)
H	8.1
C	67.2
N	2.4
O	19.9
Cl	0.1
Ca	2.3

Figure 2 shows the experimental arrangement at the deep-therapy terminal at HIRFL. Carbon ions were accelerated by HIRFL-CSRm and delivered to the therapy room. In our experiment, the standard Anderson–Braun neutron rem-meter, WENDI-2, was used. This rem-meter uses a large volume He-3 tube and has excellent energy and angular response. The neutron dose angular distribution was measured at a distance of 2 m far from the center of the tissue-like target. The size and composition of the tissue-like target is the same as the one described in the simulation model.



Fig. 2. (color online) Experimental arrangement.

3 Results and discussion

In order to obtain good statistic results, a small solid angle was taken in the present simulation for counting

the particles [16]. As shown in Fig. 1, all the solid angles used for counting are the same size. Figure 3 shows the calculated secondary neutron energy spectra and the measured data by T. Nakamura [5] as the copper target was bombarded by 400 MeV/u carbon ions. It can be seen that the FLUKA results are in good agreement with the experimental results. Because of the uncertainty of the primary ions counting, the relative results are plotted in this figure. The calculated neutron energy spectra for the tissue-like target bombarded by 430 MeV/u carbon ions is shown in Fig. 4, and the neutron dose distribution is presented in Fig. 5. The corresponding angular distribution of neutron dose is shown in Fig. 6, in which the solid line is the FLUKA result and the dots are the experimental data measured at the HIRFL deep tumor therapy terminal. Similarly, the relative results are used in this figure due to the uncertainty for counting the primary ions.

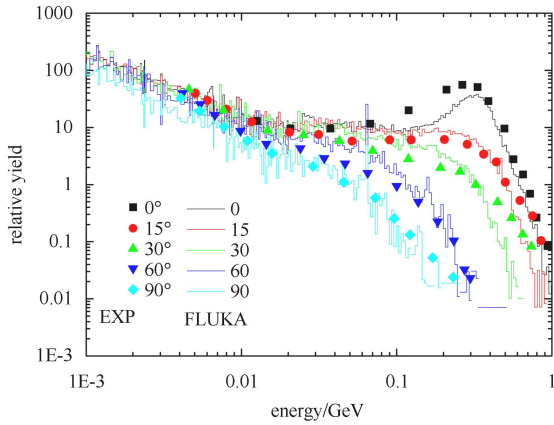


Fig. 3. (color online) Experiment data [5] and FLUKA results for a copper target bombarded by 400 MeV/u carbon ions.

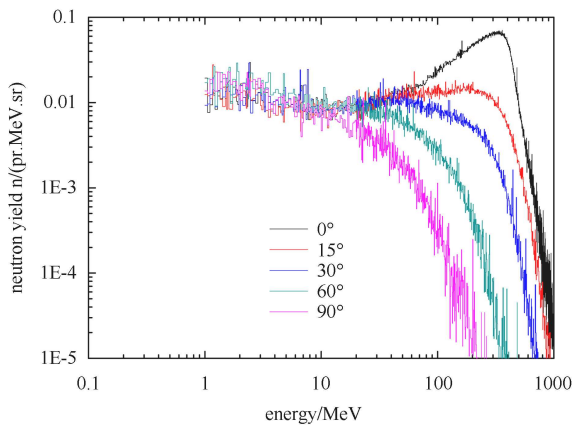


Fig. 4. (color online) Neutron spectra for a tissue-like target bombarded by 430 MeV/u carbon ions.

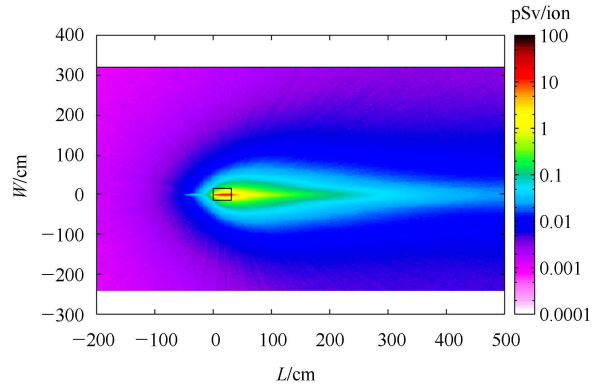


Fig. 5. (color online) Neutron dose distribution for a tissue-like target bombarded by 430 MeV/u carbon ions.

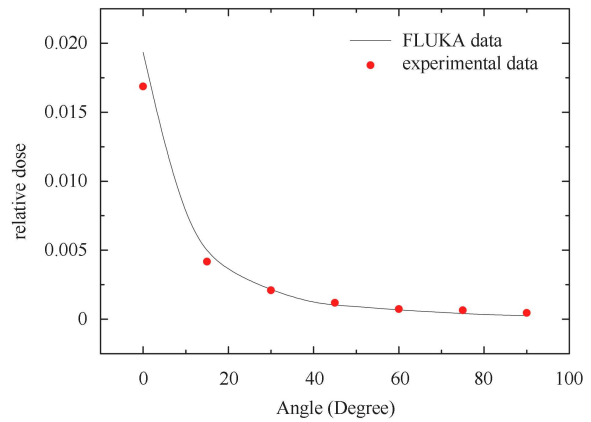


Fig. 6. (color online) Angular distribution of neutron dose for a tissue-like target bombarded by 430 MeV/u carbon ions, compared with calculated values from FLUKA.

Both Fig. 3 and Fig. 4 indicate that there is a broad peak at high energy range of the neutron spectra, especially for the zero degree situation. In this forward direction, the highest energy of the neutron achieves up to about twice as much as the incident ion energy per nucleon. As discussed in previous study [5], these high-energy neutrons are produced by a cascade process, which is the so-called pre-equilibrium process. Low energy neutrons are mainly produced in a compound nucleus system by the evaporation process. Neutron emission by the cascade process has a sharp peaking at small angles. However, the neutron spectra emitted at large angles become more gentle because the evaporation process dominates. Figure 5 shows a similar characteristic to the neutron energy spectra, i.e., the neutron dose has the largest value at zero degree and then it decreases as increasing the emitted angles. This can be explained by noting that the energy spectra can be converted to the neutron dose through the product of the appropriate flux and the dose conversion coefficients given by the ICRP.

Figure 7 shows the neutron flux density distribution inside and outside the tissue-like target. The size of this target is 30 cm \times 30 cm \times 40 cm. Inside the target, the neutron flux density first increases and then decreases along the beam direction, and far from the beam direction there are less statistics. Figure 8 shows the calculated energy deposition in the tissue-like target bombarded by 400 MeV/u carbon ions with units of GeV/cm³. In this figure, the solid line represents the total energy deposition, the dashed line represents the carbon energy deposition, and the dotted line represents the neutron energy deposition, respectively. The difference between the values represented by solid and dashed lines, especially beyond the Bragg peak, is entirely from the contribution of the fragment ions produced by nuclear reactions. The calculated results indicate that the neutron energy deposition does not exceed 1% of the carbon ion energy deposition.

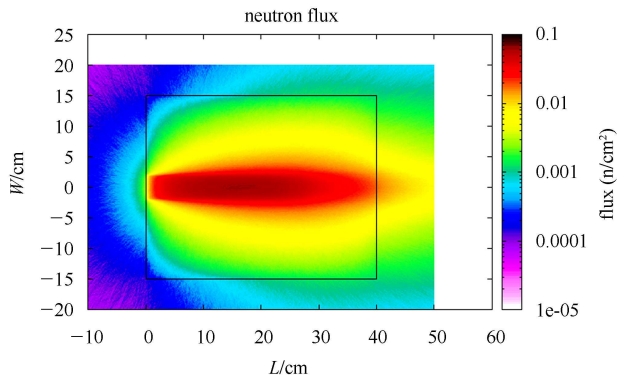


Fig. 7. (color online) Neutron flux density inside and outside the tissue-like target.

Because the Bragg peak measurements could give only the total energy deposition of all particles, and the measurements of the energy deposition from secondary neutrons is difficult inside the target, the Monte Carlo simulation is the best way to study secondary neutron energy deposition.

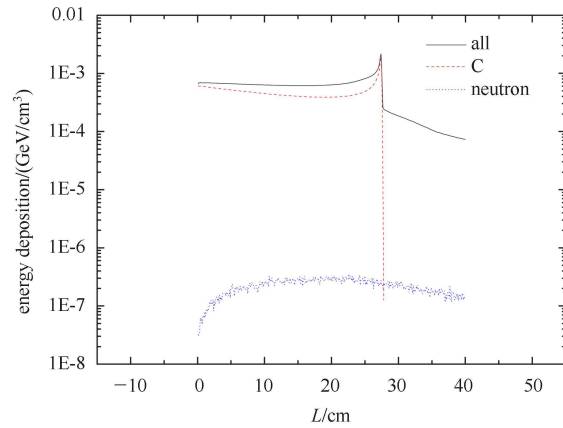


Fig. 8. (color online) Energy deposition in the tissue-like target bombarded by 400 MeV/u carbon ions.

4 Conclusions

In the present work, secondary neutron spectra for a copper target were calculated with the FLUKA code, and the results are in good agreement with previous experimental data. We then calculated the secondary neutron energy spectra and the dose distribution for the tissue-like target bombarded by carbon ions. The calculated angular distribution of the neutron dose is in good agreement with the experimental values measured at the HIRFL deep tumor treatment room. Finally, the studies show that secondary neutron energy deposition is much smaller than the total energy deposition. It is demonstrated that the neutron energy deposition is not more than 1% of the carbon ion energy deposition. These data are very important for accelerator shielding and individual dose assessment. It is found that the neutrons produced by the carbon ions do not appear to be a serious hazard to the patient body in the therapeutic process.

References

- Dieter Schardt, Thilo Elsasser Daniela Schulz-Ertner Rev. Mod. Phys., **82**: 383–425 (2010)
- ICRP Publication 74. Conversion Coefficients for use in Radiological Protection against External Radiation: Annals of the ICRP, **26**(3): 67–96 (1997)
- P. J. Taddei, J. D. Fontenot, Y. S. Zheng et al, Phys. Med. Biol., **53**: 2131–2147 (2004)
- F. Wissmann, U. Giesen, T. Klages et al, Radiat Environ Biophys, **49**: 331–336 (2010)
- T. Nakamura, N. Nakao, T. Kurosawa et al, Nuclear Science and Engineering, **132**(1): 30–57 (1999)
- M. Osipenko, M. Ripani, R. Alba et al, Nucl. Instrum. Methods A, **723**: 8–18 (2013)
- Sunil C, T. Bandyopadhyay, M. Nandy et al, Nucl. Instrum. Methods A, **721**: 21–25 (2013)
- Guisheng Li, Tianmei Zhang, Zongwei Li et al, Nucl. Instrum. Methods A, **431**: 194–200 (1999)
- Youwu Su, Zongqiang Li, Wuyuan Li et al, Chin. Phys. C, **34**(5): 548–550 (2010)
- Junkui Xu, Youwu Su, Wuyuan Li et al, Chin. Phys. C, **38**(11): 118201-1-118201-4 (2014)
- Alfredo Ferrari, Paola R. Sala, Alberto Fasso et al, *Fluka Manual*, <http://www.fluka.org/fluka.php> (2011)
- F. Ballarini, G. Battistoni, M. Campanella et al, Journal of Physics Conference Series, **41**: 151–160 (2006)
- A. Capella, U. Sukhatme, C-I Tan et al, Physics Reports, **236**(4-5): 225–329 (1994)
- H. Sorge, Phys. Rev. C, **52**(6): 3291–3212 (1995)
- M. Cavinato, E. Fabrici, E. Gadioli et al, Nucl. Phys. A, **679**: 753–764 (2001)
- D. Satoh, T. Kurosawa, T. Sato et al, Nucl. Instrum. Methods A, **583**: 507–515 (2007)